RADIANCE EMISSION BY FLARING ACTIVITY

A. Pauluhn[1] **and S.K. Solanki**[2]

[1]*International Space Science Institute, CH-3012 Bern, Switzerland, email: pauluhn@issi.unibe.ch*
[2]*Max-Planck-Institut für Aeronomie, D-37191 Katlenburg-Lindau, Germany, email: solanki@linmpi.mpg.de*

ABSTRACT

Radiance values in the quiet Sun follow a lognormal distribution, with shape and scaling parameters varying significantly over the temperature range from chromosphere to corona. We show that these distributions can be reproduced by a simple model, which assumes that the radiance is produced by a stochastic (micro-, nano-) flaring process. This allows the diagnostic capabilities of the radiance distribution to be judged, performing, e.g., estimates of the true damping times of the flares. Several energy distributions are tested for the flaring process, like a Gaussian and a power law. The resulting time series are compared with SUMER time series of equivalent sampling, after adjustment of the parameters of the simulation. A good statistical match of the measurements is obtained for a steep power law distribution of nanoflare energies.

1. INTRODUCTION

The solar emission in the EUV and X-ray wavelength ranges features transient events on all scales, e.g., flares and micro- or nanoflares, explosive events, blinkers, see, e.g., Solanki (2002) and references therein. The UV emission is often decomposed into a (nearly) steady background of emission with superposed transient brightenings (e.g., Harrison 1997; Brković et al. 2000; Innes et al. 1997). In this work we start from the basic assumption that all the emission at these wavelengths is produced by transient events (i.e., the apparent background is a superposition of many such events). We model in a very simple way time series of the radiance for a set of parameters that is consistent with the observations. The results are then statistically compared to observational data. We basically consider two representations of a data set: the first are time series of radiances, the others are probability distribution functions of radiances. In this paper we restrict ourselves to the quiet Sun. Many such transient brightenings are thought to have a common cause, namely magnetic reconnection, and via dissipation of the energy stored in the magnetic fields they provide a strong mechanism for heating the solar chromosphere and corona (Parker 1988).

The frequency or rate distribution of the energy of flares, blinkers and explosive events (dN/dE) has been found to obey a power-law for several wavelength regimes (for flares: Datlowe et al. (1974); Lin et al. (1984), for blinkers: Brković et al. (2000), for explosive events: Winebarger et al. (2002)). Flares have been the subject of a large number of studies, e.g., Krucker & Benz (1998); Parnell & Jupp (2000); Mitra-Kraev & Benz (2001); Aschwanden & Parnell (2002). Power laws have also been applied for stellar flare energy distributions, see, e.g., Audard et al. (2000); Güdel et al. (2003) and references therein. Güdel et al. (2003) compared observed and simulated distributions of EUV and X-ray measurements of the late-type active star AD Leo. They simulated light curves from model flares distributed in energy according to a power law and fitted the exponent according to the statistics of the observed lightcurves. The observed exponents α in the power-law relation $dN/dE = E_0 E^{-\alpha}$ range from 1.5 to 2.9 for solar as well as for stellar flares. Exponents within this range are also obtained for blinkers and explosive events. The larger the exponent, the more weight is given to small-scale events such as micro- and nanoflares. For an exponent greater than 2, the energy content is dominated by the small-scale events and in order to have finite total energy content, a lower cut-off in energy has to be introduced. Events in the energy range $10^{30} - 10^{33}$ erg ($10^{23} - 10^{26}$ J) are usually referred to as "normal" flares. Nanoflares (Parker 1988) are the brightenings with energy below approximately 10^{27} erg, although the limits vary somewhat in the literature. Lu & Hamilton (1991) have explained the power-law dependence of the solar flare occurrence rate in a model of self-organized criticality as avalanches of many small reconnection events.

In an earlier paper (Pauluhn et al. 2000) we have shown that the solar EUV radiance from quiet areas follows the statistics of a lognormal probability density. Here we use a stochastic model to reproduce the statistics of the quiet Sun EUV emission. We first test whether a power law distribution of flare energies results in a lognormal distribution of radiances of the modelled lightcurves. We find that this is generally the case and that the shape of the lognormal is influenced by the form of the flare distribution providing the driving input, as well as by the flare frequency and the duration or damping time of the individual flares.

We begin with an outline of the model used for the flare simulation and establish the theoretical reasoning for the radiances being lognormally distributed under the as-

Proc. of SOHO 13 'Waves, Oscillations and Small-Scale Transient Events in the Solar Atmosphere: A Joint View from SOHO and TRACE', Palma de Mallorca, Balearic Islands (Spain), 29 September – 3 October 2003 (ESA SP-547, January 2004)

sumption that they are entirely due to transient events (Sect. 2). The results of parameter studies with our model are presented in Sect. 3. In Section 4 we present a comparison with SUMER measured distributions, and the conclusions are given in Sect. 5.

2. A SIMPLE MODEL

Using a very simplified model of transient brightenings, we produce a synthetic time series of EUV radiances. We presume that flaring is an intrinsically stochastic process, and our radiance variable is a time-dependent stochastic (or random) variable, i.e., a stochastic process. One simulation thus delivers a possible realization of this process. Our model simply consists of a time series of random kicks (acting as "flares"), applied to an initial value (whose exact value is not important, since it is damped just like every brightening and the model will reach a kind of "steady state" after a certain relaxation time). Each kick is followed by the exponential decay of the radiance. The final radiance is given by the sum of the radiances of all the overlapping transient brightenings.
Depending on the choice of the temporal profile of a single brightening event we have either 5 or 6 free parameters: the flare amplitude range and the power-law exponent, the e-folding or damping time of the flare, if we assume a single kick with a sharp rise and a successive exponential decrease. Additionally, in order to smooth the steep increase a rise time can be introduced. Furthermore, the frequency of the excitation, i.e., the flaring rate or flaring probability p_f, has to be determined. We start with some general considerations and the description of the model setup and then present a theoretical derivation for the most simple case of our stochastic model.

2.1. The simulation

The model produces realizations of possible radiance time series, i.e., we get the radiance as a time-dependent stochastic variable (stochastic process), and it describes an example of a process which is close to being Markovian. In a Markov process, the stochastic variable at one timestep t_{n+1} is only dependent on the directly preceding timestep t_n. It has "nearly no memory" of the history, and the probability to find a variable at position x_{n+1} at time t_{n+1} is calculated by an initial probability and the two-time transition probability (which is the conditional probability that the variable is in state x_{n+1} at t_{n+1} under the condition that it has been in state x_n at t_n).

The simulation involves the following steps:

1. Generate a distribution of flare sizes, i.e. (positive) values of flare amplitudes f_n.
2. Start from an initial radiance value $r_0 > 0$ (this can be the "first kick" from the flare distribution, $r_0 = f_0$).
3. At random time t_i another radiance r_i is generated by adding a flare kick f_i,
$$r_i = r_{i-1} + f_i. \quad (1)$$
4. At successive time steps t_j, $j > i$, the radiance values are
$$r_j = r_i \cdot \exp(-\frac{t_j - t_i}{\tau_D}), \quad (2)$$
with τ_D the damping time, again multiplicatively generated from the preceding values. Here we assume for simplicity that all brightening events have the same damping time and that there is no correlation between, e.g., damping time and amplitude.

The probability of a transient brightening occurring, p_f with $0 < p_f < 1$, is simulated by drawing equally distributed random numbers between 0 and 1, and a flare event is started at t_i if the random number falls within a certain fraction of the interval (0,1), e.g., a flaring probability of 30 % or 0.3 is realized by applying the kick if the random number is smaller than 0.3.

We assume that we can express the kick as $f_i = c \cdot r_{i-1}$, with $c = \frac{f_i}{r_{i-1}}$ a positive value, i.e., the new radiance is

$$r_i = r_{i-1} + c \cdot r_{i-1} = \hat{c} \cdot r_{i-1}, \quad (3)$$

a multiple of the predecessor radiance. We stress, however, that we prescribe the distribution of the additive components f_i (given, e.g., by observation as a power law) and not that of the multiplicative component c.

Thus, the radiance value at the nth step is

$$r_n = r_0 \cdot c_1 \cdot c_2 \cdot \cdots \cdot c_n, \quad (4)$$

with the c_i being random factors if a new kick happens at this time. Otherwise c_i represents the damping as described by the exponential in Eq. (2).

Taking the logarithm of this equation yields

$$\log(r_n) = \log(r_0) + \log(c_1) + \log(c_2) + \cdots + \log(c_n). \quad (5)$$

The Central Limit Theorem (applied to the logarithms, which are itself independent random variables, if the c_i are independent) then states that as n goes to infinity, the distribution of the sum converges to a normal distribution. Thus, the distribution of the sum in Eq. (5) is normal, so that the distribution of the r_n is lognormal. The next step is the determination of the parameters of the lognormal distribution

$$\rho(x) = \frac{N_0}{\sigma_l x \sqrt{2\pi}} \exp(-\frac{(\log(x) - \mu_l)^2}{2\sigma_l^2}) \quad (6)$$

with $\mu_l = <\log(x)>$, $\sigma_l = \sqrt{Var(\log(x))}$ and N_0 a normalization factor.

2.2. An analytic model

Provided the assumption holds, an analytic model can be developed, based on a stochastic differential equation (SDE) for the radiance variable and its corresponding partial differential equation for the probability density, the Fokker-Planck equation (FPE, see, e.g., Risken

1989; Gardiner 1990; Honerkamp 1990).
We start with a linear SDE with only two free parameters, which we will later relate to damping and excitation, both represented by the flaring process, and determine their values empirically, i.e., via model runs and parameter scans.
Let now r be the radiance variable, and F the stochastic flare process, which stands for the noise, i.e., the randomness, in the equation. Our model computes the following:

$$\mathrm{d}r = r \cdot \mathrm{d}F. \tag{7}$$

This equation can be seen as an SDE with so-called "multiplicative" noise (e.g., Gardiner 1990; Honerkamp 1990). Substituting $x = \log(r)$ (which is unproblematic in our case of stochastic calculus, see, e.g., Gardiner 1990), we get:

$$\mathrm{d}x = \mathrm{d}F \tag{8}$$

This is an equation of much nicer type because the diffusion term is independent of x.

The stochastic process $F(t)$ is neither a White Noise process $\xi(t)$ (which means that it is totally uncorrelated with $< \xi(t)\xi(t') >= \delta(t - t')$) nor does it have mean zero. However, the coloured noise process F is generated from White Noise by the following equation

$$\mathrm{d}F = \mathrm{d}x = (-kx + c)\mathrm{d}t + b\mathrm{d}W, \tag{9}$$

with W the White Noise process and $k = \frac{1}{\tau_D}$ the damping parameter.

Our free parameters in the model equation are a deterministic offset c and the effective noise strength b.
For our model, we determined the two parameters via parameter scans as functions of τ_D and p_f.

An equation of the form (9) is equivalent to the FPE

$$\frac{\partial \rho}{\partial t} = \frac{\partial}{\partial x}(kx - c)\rho + \frac{1}{2}\frac{\partial^2}{\partial x^2}b^2\rho. \tag{10}$$

As the first coefficient on the right-hand side is a linear function in x and the diffusion coefficient (b^2) is independent of x, it is solvable. The solution is given by a Gaussian process and as such completely determined by its mean and variance

$$\rho(x,t) = \frac{1}{\sqrt{2\pi}}\frac{1}{\sqrt{\frac{b^2}{2k}(1-\exp(-2kt))}} \cdot \exp\left(-\frac{1}{2}\frac{(x - x_0\exp(-kt) - \frac{c}{k})^2}{\frac{b^2}{2k}(1-\exp(-2kt))}\right) \tag{11}$$

with the boundary condition $\rho(x, 0|x_0, 0) = \delta(x - x_0)$.

For $t \to \infty$ it approaches the stationary solution ($\frac{\partial}{\partial t}\rho = 0$)

$$\rho_{stat}(x) = \frac{1}{\sqrt{2\pi}}\frac{1}{\sigma_g}\exp\left(-\frac{1}{2}\frac{(x-\mu_g)^2}{\sigma_g^2}\right), \tag{12}$$

where we have set $\mu_g = \frac{c}{k}$ and $\sigma_g = \frac{b}{\sqrt{2k}}$.

The logarithm of the radiance $\log(r)$ is thus Gaussian distributed, and consequently the radiance r follows a lognormal distribution. The parameters μ_g and σ_g correspond to the μ_l and σ_l in (6).

On the time scales under study (several hours), we can assume stationarity of our distribution, which means that (after a relaxation time in the model) a steady state is reached. This does not hold for the solar radiance over longer periods, exceeding time scales of months to years, e.g., a dependence of the shape of distribution on the solar cycle is expected. This would also apply for shorter time scales when the structure of the region changes significantly, e.g., by emergence of new flux and thus a change in activity.

In principle, the model is, in logarithmic space, similar to a Brownian motion model (Einstein 1905; Langevin 1908; von Smoluchowski 1915), but with smoother paths of the realizations due to the damping. A pure Brownian motion is represented by the diffusion equation

$$\frac{\partial}{\partial t}\rho = D\frac{\partial^2}{\partial x^2}\rho, \tag{13}$$

with a diffusion coefficient D. Such a diffusion type of model has for example also been successfully applied to the distribution of the logarithms of file sizes on server systems (Downey 2001). However, undamped Brownian motion represents the Wiener process, and no stationary solution exists.

The two characterizing parameters of the stationary solution (12), μ_g and σ_g, have been determined empirically by parameter scans for Gaussian and for power-law noise input.

3. RESULTS

We determined the parameters of the radiance distribution via the simulation of a number of time series (each of $n = 5 \cdot 10^5$ time steps) for several damping times and flare-probabilities (i.e., kick-frequencies), respectively. We ran the model using two different distributions for the amplitudes of the stochastic flaring process as input: 1. kicks with Gaussian-distributed amplitudes ($\mathcal{N}(0.09, 0.02)$), 2. kick amplitudes which are distributed according to a power-law, with the exponent $\alpha = -2.1$ and the amplitude range between 0.02 and 3.0 $\mathrm{W\,m^{-2}sr^{-1}}$. The first two moments of the resulting distributions have been chosen to be equal for the Gaussian and the power-law: a mean m_f of 0.09 and a standard deviation σ_f of 0.02.

All simulated radiance time series were lognormally distributed. Figure 1 shows examples of simulated distributions with damping times $\tau_D = 10, 50, 100$ and 200 time steps, and a flaring frequency of $p_f = 0.2$. Both curves (for Gaussian and for power-law distributed flare excitation) have been plotted. Clearly, the resulting distributions are highly skewed towards small radiances for a

short damping time. In the limit of infinitely short damping time the most common value of the radiance is zero. As the damping time increases, so do the average value and the width of the radiance distribution, which also becomes increasingly symmetric. The same behaviour is found as the flare frequency increases.

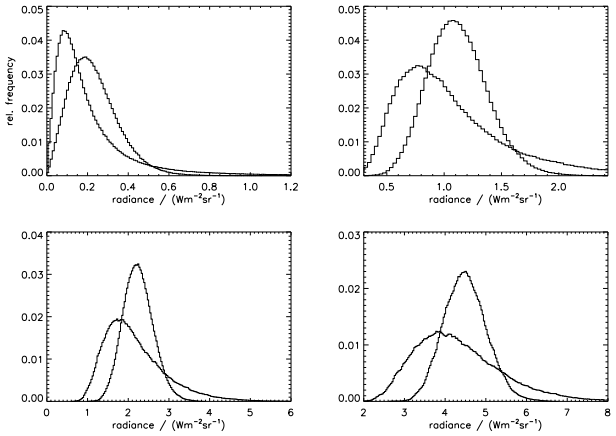

Figure 1. Histograms of the simulations with τ_D =10, 50, 100, and 200 for a fixed flaring probability of 0.2. The thin curves show the radiance frequency distributions for the Gaussian flare distribution as input and the thick curves for the power-law input.

3.1. Variation of the damping time and flaring frequency

We varied the damping time (in units of time steps) from 5 to 500 and kept the flaring probability p_f fixed. The two parameters characterizing the resulting lognormal distributions are shown in Fig. 2 for a Gaussian flare distribution and $p_f = 0.2$.

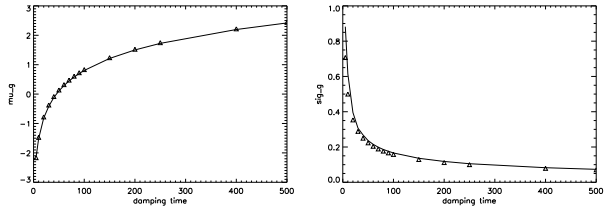

Figure 2. Variation of the lognormal parameters with damping time for a fixed flaring probability of 0.2 and a Gaussian flare distribution. The solid lines show the modelled curves, the triangles show the values calculated with Eqs. (14) and (15).

The variation of the lognormal parameters with flaring frequency is shown in Fig. 3.

The values of the lognormal parameters which fitted the model simulations were

$$\mu_g = \log(\tau_D m_f p_f) + p_f \exp(p_f) = \log(\tau_D f(m_f, p_f)), \quad (14)$$

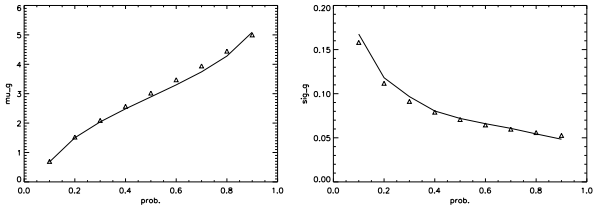

Figure 3. Variation of the lognormal parameters with flaring probability for a fixed damping time of 200 time steps and a Gaussian flare distribution. The solid lines show the modelled curves, the triangles show the values calculated with Eqs. (14) and (15).

with $f(m_f, p_f) = m_f p_f \exp(p_f \exp(p_f))$, and

$$\sqrt{2}\sigma_g = \frac{1}{\sqrt{\tau_D p_f}}. \quad (15)$$

We checked for an influence of the standard variation σ_f of the flare distribution on the parameters and found that for a doubled value $\sigma_f = 0.04$, only the σ_g was slightly higher by approximately 4 %. However, we did not determine a possible weak functional dependence $\tilde{f}(\sigma_f)$. A more general expression for σ_g thus might read $\sigma_g = \frac{\tilde{f}(\sigma_f)}{\sqrt{2\tau_D p_f}}$.

For a power-law distributed flare input the μ_g of the resulting distribution is the same, the σ_g of the distribution, however, is larger by a factor of 2 for $p_f < 0.5$. With increasing flare frequency ($p_f \geq 0.5$) the factor reduces to 1.2 for $p_f = 0.9$. (The σ_g approaches that of a Gaussian noise input for increasing noise frequency.)

The Fokker-Planck equation (10) for our model is thus

$$\frac{\partial \rho}{\partial t} = \frac{\partial}{\partial x}\left(\frac{1}{\tau_D}x - \frac{\log(\tau_D f(m_f, p_f))}{\tau_D}\right)\rho + \frac{1}{2\tau_D^2 p_f}\frac{\partial^2}{\partial x^2}\rho. \quad (16)$$

4. COMPARISON WITH SUMER DATA

Having established a theoretical model for a very simple case, as a next step we try to find a set of parameters for a representation of SUMER data from the transition region. We use a power-law distributed flaring process and additionally introduce a possible rise time of a flare τ_R. Instead of instantaneous increase and exponential decay the flare brightness can now both, rise and fall exponentially. The simulation consisted of $n = 24\,000$ time steps.

4.1. The SUMER data

SUMER is a stigmatic normal incidence telescope and spectrometer, operating in the wavelength range from 465 to 1610 Å, depending on the spectral order and the choice of detector. For a general description of the SUMER instrument and its data we refer to Wilhelm et al. (1995).

The SUMER slit with angular dimensions of $1'' \times 300''$ is imaged by the spectrograph on to the detectors with a resolution of about $1''$ per pixel in the spatial direction and 0.044 Å per spectral pixel in first order and 0.022 Å per spectral pixel in second order.
The Si IV line at 1393 Å, which is used here, is measured in first order. Its origin lies in the transition region ($T \approx 10^5$ K), and thus features high variability. The measurements belong to a quiet Sun explosive events study, they have been made over 3 h and 35 min on 19 July 1998 with a cadence of 15 s and have a spatial resolution of $2''$. The SUMER data were corrected for the flatfield, the geometric distortion, and for detector electronics effects such as dead-time and local-gain depression.
After the instrumental corrections and the radiometric calibration, the solar radiances were determined by integration over the line profiles, which were derived by least-squares fits of single Gaussian functions and a linear background. The background (continuum) was subtracted prior to integration.

4.2. Model lightcurves and comparisons with the data

Figure 4 shows two sample histograms from lightcurves of the SUMER data, the first from a darker area of the images (cells), the second from a brighter part (network). In 4 (a) the histogram of a 1-pixel time series (from a $1'' \times 2''$cell area) is given, together with the result of a simulation with the parameters $\alpha = 3.0$, amplitude range of the flare-kicks $0.01 - 0.3$ W m^{-2} sr^{-1}, damping time $\tau_D = 28$ time steps à 15 s (if compared to the SUMER temporal sampling), rise time of $\tau_R = 21$ time steps, and a flare probability $p_f = 0.2$. In 4 (b) the respective two histograms are given for a network area of same size. The parameters of the simulation were $\alpha = 3.0$, amplitude range of the flare-kicks $0.6 - 3.0$ W m^{-2} sr^{-1}, damping time $\tau_D = 7$ time steps, rise time of $\tau_R = 5$ time steps à 15 s, and a flare probability $p_f = 0.2$. The agreement between measured and modelled histograms is quite reasonable, although not all features of the measured histograms are captured well, e.g., the steep increase at lower radiances is not shown by the simulations. Some of the differences, however, can be ascribed to the better statistics of the model (24 000 data points compared to SUMER's 821).

Figure 5 shows for comparison a time series of an area of $1'' \times 2''$of the SUMER measurements and a part of the simulated lightcurve for a network area. A Poisson photon noise (of 5 %) has been added to the synthetic lightcurve to simulate photon noise. Although the main statistical properties of the SUMER data are well represented (see Fig. 4), there are significant differences visible in the two lightcurves. Especially, the lower limit or background is not captured well by the simulation. The opposite is the case for a cell area simulation: what is given by the weakly damped process (compare the large $\tau_D + \tau_R$ for the simulation shown in Fig. 4 (a)) is mainly the background. Single higher-intensity events appearing in the tail of the distribution of Fig. 4 (a) are not covered.

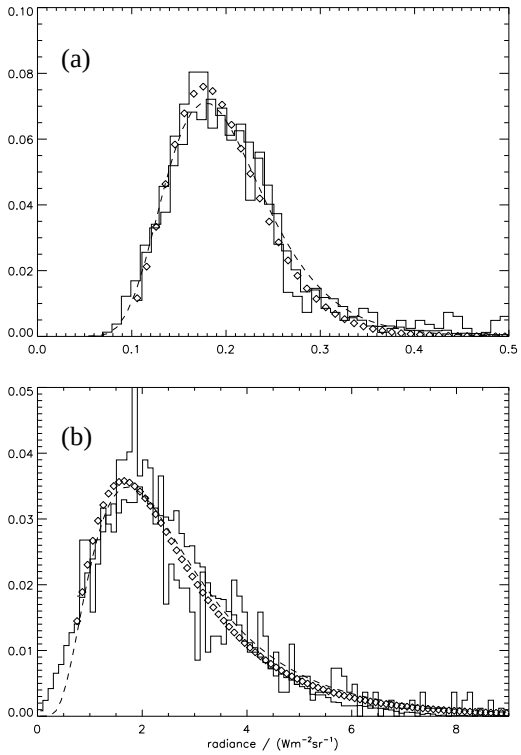

Figure 4. Histograms of the simulated and SUMER measured radiances. (a): from a time series in a very quiet area (cells). (b): from network area of the same size ($1'' \times 2''$). The thin histogram and dashed line give the data and fit of the simulation, the thick histogram and the diamonds show the corresponding values for the SUMER measurements.

4.3. Discussion

From the multiplicative version of the central limit theorem it follows that the product of many independent, identically distributed, positive random variables has approximately a lognormal distribution. (For a discussion of the special features of the lognormal distribution function see also, e.g., Limpert et al. (2001).) For a lognormal to form in the simulation, the input process has to be positive definite, e.g., a Gaussian with mean zero as input distribution does not produce a lognormal. Thus, by the positive input process, the asymmetric shape is ensured.

The shape and scale of the resulting lognormal are strongly dependent on the damping time of the flares and their frequency. The higher the flaring frequency and the damping time, the more symmetric the resulting lognormal becomes (i.e., the σ_g values which determine the shape of the lognormal become smaller). With increasing frequency and damping time, the lognormal becomes more Gaussian-like, decreasing damping time (i.e., stronger damping) and more frequent flares introduce more asymmetry, and make the mode (i.e., the peak or most frequent value) of the radiance distribution approach zero. The scaling of the distribution, which is its extension in (peak-) height and width, is given by μ_g. μ_g increases with damping time (i.e., with decreasing damp-

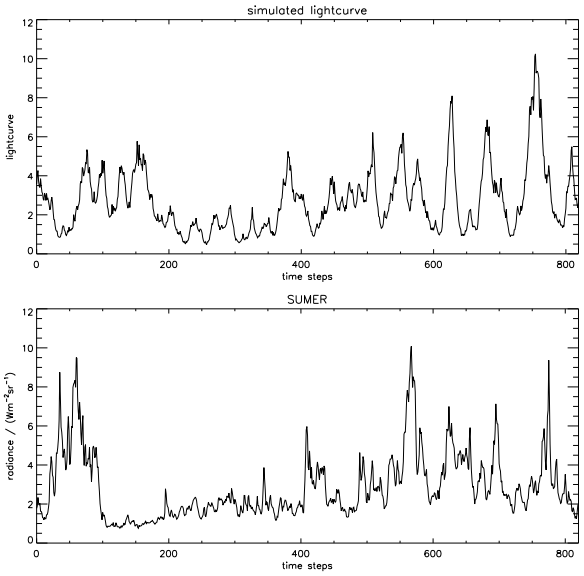

Figure 5. Time series of radiances simulated with a power-law of $\alpha = 3$, amplitude range between 0.6 and 3.0 $W m^{-2} sr^{-1}$, a damping time of $\tau_D = 7$ time steps, a rise time of $\tau_R = 5$ time steps, $p_f = 0.2$, and a SUMER lightcurve from a network part of the images.

ing) and with flaring frequency.
Comparing the analytical expression for σ_g with Figs. 6 and 7 from Pauluhn et al. (2000), which show that the shape parameter of the lognormal as a function of temperature has a maximum at the transition region, it seems that flaring time scales there are relatively shorter than in chromosphere and corona, or the flare frequency is lower there.
Our simulations show that multiplicative stochastic processes are suitable models for solar transient brightenings. From Figs. 4 and 5 it further follows that a single flaring process is not enough to fully represent a SUMER transition region time series. In order to cover "background flaring" as well as flaring with higher amplitude, a superposition of two or more processes with different time scales and amplitudes is needed. This result may be an artifact of the fact that we assume the damping time to be independent of the amplitude of the brightening, while in reality there could be a connection (e.g., an inverse correlation).

5. SUMMARY AND CONCLUSIONS

We have shown that a simple model of randomly generating a time series of radiances by (flare-)excitation can approximately reproduce measured quiet Sun statistics. An analytical background for the lognormal distribution of quiet Sun radiances was given, and it was shown that the probability density function of the logarithm of the radiance obeys a diffusion law in the case that the radiance process can be seen as multiplicative.
For simple sample cases, we determined the functional dependence of the stationary radiance distribution on the parameters of the flaring process, such as the flare frequency and the flare damping time.

We have not explicitly studied the dependence on the parameter α of the power-law input distribution, although it enters, together with the amplitude range of the input, via the mean value. Certainly more studies are required to refine the approximate equations and dependences, as well as to include superpositions of processes. Also, comparisons with long time series of different temperature regions should be undertaken.

ACKNOWLEDGEMENTS

SOHO is a project of international cooperation between ESA and NASA.

REFERENCES

Audard, M., Güdel, M., Drake, J.J., & Kashyap, V.L. 2000, *Astrophys. J.*, 541, 396

Aschwanden, M.J., & Parnell, C.E. 2002, *Astrophys. J.*, 572, 1048

Brković, A., Solanki, S. K., & Rüedi, I. 2001, *A&A*, 373, 1056

Datlowe, D.W., Elcan, M.J., & Hudson, H.S. 1974, *Sol. Phys.*, 39, 155

Downey, A.B. 2001, The structural cause of file size distributions, *IEEE MASCOTS'01*, 361

Einstein, A. 1905, *Ann. Phys.*, 17, 549

Gardiner, C.W. 1990, *Handbook of Stochastic Methods*, 2nd edition, Springer-Verlag, New York, Berlin, Heidelberg

Güdel, M., Audard, M., Drake, J. J., Kashyap, V. L. & Guinan, E. F. 2003, *Astrophys. J.*, 582, 423

Harrison, R. A. 1997, *Sol. Phys.*, 175, 467

Honerkamp, J. 1990, *Stochastische Dynamische Systeme*, VCH, Weinheim, Germany

Innes, D. E., Inhester, B., Axford, W. I., Wilhelm, K. 1997, *Nature*, 386, 811

Krucker, S., & Benz, A.O. 1998, *Astrophys. J.*, 501, L213

Langevin, P. 1908, *Comptes. Rendues*, 146, 530

Limpert, E., Stahel, W.A., & Abbt, M. 2001, *BioScience*, 51/5, 341

Lin, R.P., Schwartz, R.A., Kane, S.R., Pelling, R.M., & Hurley, K.C. 1984, *Astrophys. J.*, 283, 421

Lu, E.T., Hamilton, R.J. 1991, *Astrophys. J.*, 380, L89

Mitra-Kraev, U., Benz, A.O. 2000, *A&A*, 373, 318

Parker, E.N. 1988, *Astrophys. J.*, 330, 474

Parnell, C.E., & Jupp, P.E. 2000, *Astrophys. J.*, 529, 554

Pauluhn, A., Solanki, S.K., Rüedi, I., Landi, E., & Schühle, U. 2000, *A&A*, 362, 737

Risken, H. 1989, *The Fokker-Planck Equation*, 2nd edition, Springer-Verlag, New York, Berlin, Heidelberg

von Smoluchowski, M. 1915, *Phys. Z.*, 16, 321

Solanki, S.K. 2002, *ISSI Sci. Rep. SR-002*, eds. A. Pauluhn, M.C.E. Huber, & R. von Steiger, 1

Winebarger, A. R., Emslie, A. G., Mariska, J. T., & Warren, H. P. 2002, *Astrophys. J.*, 565, 1298

Wilhelm, K., Curdt, W., Marsch, E., et al. 1995, *Sol. Phys.*, 162, 189